PROTEINS: Structure, Function, and Bioinformatics 67:1119–1127 (2007)

Site Directed Mutagenesis at Position 193 of Human Trypsin 4 Alters the Rate of Conformational Change During Activation: Role of Local Internal Viscosity in Protein Dynamics

Júlia Tóth, Zoltán Simon, Péter Medveczky, Linda Gombos, Balázs Jelinek, László Szilágyi, László Gráf,* and András Málnási-Csizmadia*

Department of Biochemistry, Institute of Biology, Eötvös Loránd University, H-1117 Budapest, Hungary

ABSTRACT **Upon activation of trypsinogen four peptide segments flanked by hinge glycine residues undergo conformational changes. To test whether the degree of conformational freedom of hinge regions affects the rate of activation, we introduced amino acid side chains of different characters at one of the hinges (position 193) and studied their effects on the rate constant of the conformational change. This structural rearrangement leading to activation was triggered by a pH-jump and monitored by intrinsic fluorescence change in the stopped-flow apparatus. We found that an increase in the size of the side chain at position 193 is associated with the decrease of the reaction rate constant. To analyze the thermodynamics of the reaction, temperature dependence of the reaction rate constants was examined in a wide temperature range (5–60°C) using a novel temperature-jump/stopped-flow apparatus developed in our laboratory. Our data show that the mutations do not affect the activation energy (the exponential term) of the reaction, but they significantly alter the preexponential term of the Arrhenius equation. The effect of solvent viscosity on the rate constants of the conformational change during activation of the wild type enzyme and its R193G and R193A mutants was determined and evaluated on the basis of Kramers' theory. Based on this we propose that the reaction rate of this conformational transition is regulated by the internal molecular friction, which can be specifically modulated by mutagenesis in the hinge region. Proteins 2007;67:1119–1127.**

Key words: trypsinogen activation; structural rearrangement; trypsin; Arrhenius plot; Kramers' theory; pH-jump; temperature-jump/stopped-flow

INTRODUCTION

Trypsin is a prototype of the S1 family of the serine proteases, and is synthesized in an inactive zymogen form. Zymogens are activated by proteolytic cleavage of the activation peptide. The α-amino group of the newly formed N terminus, Ile16 (chymotrypsinogen numbering) forms a stabilizing salt bridge with the Asp194 side chain carboxylate group, which triggers a conformational change leading to the active enzyme.[1–3] This structural change affects a distinct region of the protein comprising 15% of the molecule, while 85% of the structures of the zymogen and the active enzyme are identical (Fig. 1). Four peptide segments undergo conformational rearrangement that involve segments 16–19, 142–152 (the autolysis loop), 184–194, and 216–223 (these latter two form the substrate binding pocket and the oxyanion hole) collectively referred to as the activation domain.[3] The conformational change completes formation of the oxyanion hole comprising the amido groups of Gly193 and Ser195 and the substrate binding pocket.[5,6]

The conformational change upon activation can also be triggered by a pH-jump from pH 11.0 to pH 8.0[7–9] and monitored by measuring the intrinsic fluorescence of the enzyme,[10] offering an elegant experimental approach to study the structural rearrangement. It was shown for chymotrypsin that the rate constants measured by the pH-jump method are in excellent agreement with the data acquired from proflavine binding studies.[10,11]

Targeted molecular dynamics simulations of trypsinogen to trypsin transition showed that the largest changes in main chain dihedral angles occur at certain

Abbreviations: CABS, 4-(Cyclohexylamino)-1-butanesulfonic acid; DMF, dimethylformamide; k_{cat}, catalytic constant; K_m, Michaelis constant; NATA, *N*-acetyl L-tryptophan amide, Z-Gly-Pro-Arg-pNA, *N*-carbobenzyloxy-glycyl-prolyl-arginyl *p*-nitroanilide; Tricine, *N*-[2-hydroxy-1,1-bis(hydroxymethyl)ethyl]glycine.

Grant sponsor: Hungarian Scientific Research Fund; Grant numbers: OTKA TS49812 and TS047154; Grant sponsor: European Molecular Biology Organization (EMBO); Grant sponsor: Howard Hughes Medical Institute (HHMI); Grant sponsor: National Office for Research and Technology; Grant number: RET 14/2005.

The first two authors contributed equally to this paper.

*Correspondence to: László Gráf and András Málnási-Csizmadia, Department of Biochemistry, Institute of Biology, Eötvös Loránd University, Pázmány Péter sétány 1/C, H-1117 Budapest, Hungary. E-mail: malna@elte.hu

Received 11 July 2006; Revised 19 October 2006; Accepted 22 December 2006

Published online 13 April 2007 in Wiley InterScience (www.interscience.wiley.com). DOI: 10.1002/prot.21398

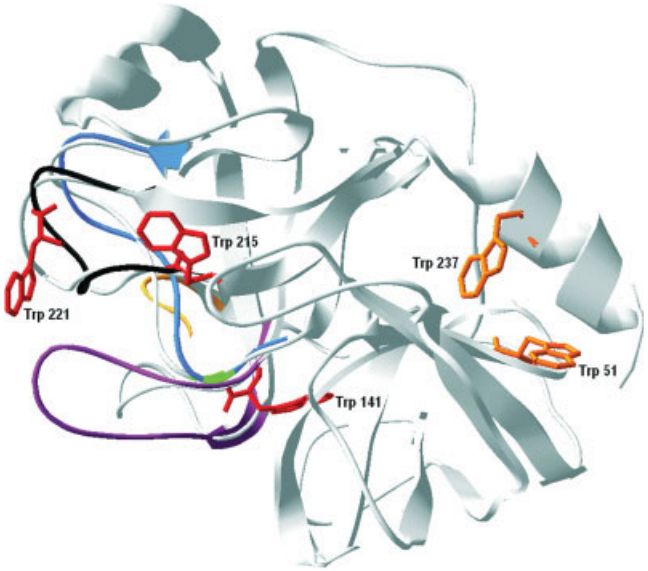

Fig. 1. Superimposed structure of bovine trypsinogen (PDB ID: 1tgn) and human trypsin 4 (PDB ID: 1h4w) visualized using software DeepView-spdv 3.7.[4] The peptide backbone segment of human trypsin 4 whose conformation differs from the conformation of bovine trypsinogen (gray) corresponding to the activation domain is shown as a colored ribbon. The 16–19 peptide segment is shown in yellow, the 142–152 segment is colored purple, and the 184–194 and 216–223 segments are represented by a blue and a black ribbon, respectively. The backbone of residue 193, which goes through large dihedral angle transition in the course of activation is shown in green. Tryptophan residues are also highlighted, Trp141, 215 and 221 that might account for the fluorescence intensity change during the conformational change are colored red, while Trp51 and Trp237 is shown in orange (chymotrypsin numbering system is used to identify the residues).

glycine residues among which Gly19, Gly142, Gly184, Gly193, and Gly216 border the activation domain peptides.[12] These glycine residues exhibit larger Φ and/or Ψ angle changes than the surrounding residues. This suggests that these glycines have a well-defined role in the activation process: they act as hinges for the conformational change and the four peptide segments move as more rigid units.[10,12] The presence of glycines at conserved positions of the activation domain seems to promote the conformational transition. As a consequence, replacement of Gly193, which is one of the hinge residues by an amino acid possessing a bulky and/or charged side chain is supposed to have significant effect on the rate and thermodynamics of the conformational change upon activation. This phenomenon can be interpreted according to Kramers' rate theory. Position 193 is well conserved among serine proteases: it is occupied by a glycine residue except for rare examples. One of these exceptional enzymes is human trypsin 4 possessing an arginine at this position.

On the basis of recent molecular dynamics and targeted molecular dynamic simulations, the sequence of the main substeps upon activation of bovine and rat chymotrypsinogen was deduced.[13,14] In the study of Mátrai and coworkers, the role of Gly193 in the sequence of events was also described. The conformational changes in the backbone of position 192 trigger the reorientation of Gly193 towards the substrate binding site and a rotation around the C_α—C bond of Asp194 of approximately 180°. As a consequence, a cavity is left behind, which is necessary for the penetration of Ile16 into the core of the molecule and allows formation of the salt bridge between the α-amino group of Ile16 (the N-terminus of trypsin) and the side chain carboxylate group of Asp194. The series of events leads to an active enzyme conformation possessing the substrate binding pocket and oxyanion hole necessary for efficient enzymatic activity.

The aim of this work was to study the effect of point mutations in the hinge on the rate of the conformational change and characterize the thermodynamics of this structural rearrangement. We sought for an experimental system where this change in the protein conformation is a single-step first-order transition, which is accompanied by an intrinsic signal change in the protein. The rearrangement of the activation domain of serine proteases upon activation meets all these criteria. Human trypsin 4 and its site 193 variants were chosen to be analyzed, as this enzyme is biochemically well characterized[15–19] and its three dimensional structure has been determined.[20] We expressed wild type human trypsinogen 4 and its R193G/A/Y/F mutants and monitored their conformational change upon activation in pH-jump stopped-flow experiments detecting the intrinsic fluorescence change. We found that this conformational transition is affected by the mutations at position 193, and that its rate constant decreases with the size of the sidechain. We also studied the temperature dependence of the rate constant of the transition in the 5–38°C range with a conventional stopped-flow apparatus. Furthermore, we developed a new temperature-jump/stopped-flow setup,[21] which allowed the extension of the Arrhenius plots up to 60°C. The main advantage of this setup is that fast temperature-jump occurs simultaneously with rapid mixing of the reactants, thus the dead time does not increase compared with a conventional stopped-flow apparatus. With this novel temperature-jump/stopped-flow instrument kinetics of reactions can be monitored at high temperatures, even above the denaturation temperature of the protein if the monitored reaction steps are faster than the generally slow heat denaturation reaction.

Thermodynamic analysis revealed that these mutants differ only in the pre-exponential term of the Arrhenius equation, and the activation energy is unaffected by the mutations. The rate of the conformational transition of the wild type enzyme and its R193G and R193A mutant was measured in buffers of different relative viscosity, and we found that the rate of the conformational transition is inversely proportional to the solvent viscosity. This phenomenon is interpreted in terms of the Kramers' theory. On the basis of the work of Ansari et al.[22] a parameter with units of viscosity is introduced, called internal viscosity, which can be regarded as a contribution of the protein friction to the total friction. We conclude that the rate of conformational change during activation of trypsinogen site 193 mutants is determined by the internal molecular viscosity around this hinge site.

MATERIALS AND METHODS

Mutagenesis and Expression of Human Trypsinogen 4 Variants

Wild type human trypsinogen 4 was cloned as described previously.[20] The R193G mutant clone was generated as reported by Tóth et al.[18] The amino acid substitutions at position 193 were generated by the megaprimer mutagenesis method using the following oligonucleotides: hTry4_R193A: 5′ TCC TGC CAG GCT GAC TCC GGT GGC 3′, hTry4_R193F: 5′ TCC TGC CAG TTT GAC TCT GGT GGC CC 3′, and hTry4_R193Y: 5′ TCC TGC CAG TAT GAC TCT GGT GGC CC 3′ (Invitrogen, Carlsbad, CA). The PCR products were ligated to pBluescript vector *via* TA-ligation and were sequenced. Mutant genes were subcloned into a modified pET-17b vector utilizing the HindIII and SacI cleavage sites introduced by the 3′ and 5′ oligonucleotides.[20] Trypsinogens were expressed, renatured[15] and activated, purified and purity was assessed[18] as described previously. The enzymes were dialyzed against 2.5 m*M* HCl and stored at −20°C. The concentration of the prepared enzymes were determined by active site titration with 4-methylumbelliferyl 4-guanidinobenzoate[23] (Sigma-Aldrich, St. Louis, MO), or based on their absorbance at 280 nm using the theoretical extinction coefficient $\varepsilon_{280} = 40570\ M^{-1}\ \mathrm{cm}^{-1}$.

Steady State Kinetic Measurements

Determination of k_{cat} and K_m

Measurements were carried out with 0.5–2 n*M* enzymes on Z-Gly-Pro-Arg-pNA substrate (Sigma-Aldrich Co., St. Louis, MO) in 50 m*M* Tricine (Sigma-Aldrich Co., St. Louis, MO), 10 m*M* $CaCl_2$ pH 8.0 buffer at 20.0°C. Substrate stock solutions were prepared in dimethylformamide, and the final concentration of DMF in the assays was less than 1%. Hydrolysis of the substrate was monitored by measuring the generation of the paranitroanilin product at 405 nm using a Shimadzu UV-2101PC spectrophotometer. Initial velocities were measured at six different substrate concentrations in the range of 5–250 μ*M*. Three parallel measurements were carried out for each data points. The values of k_{cat}, K_m, and k_{cat}/K_m were determined from the parameters of the hyperbolas fitted to the initial velocities plotted against substrate concentration.

Transient Kinetic Measurements

Stopped-flow measurements

Transients were recorded on a SF-2004 instrument (KinTek, Austin, TX) equipped with a 450-W Hg-Xe super-quiet lamp (Hamamatsu Photonics UK, Welwyn Garden City, United Kingdom). Tryptophans were excited at 297 nm with a bandwidth of 2 nm and fluorescent emission was detected with a photomultiplier set to 700 V through a 340 nm interference filter (Comar Instruments, Cambridge, United Kingdom). The dead time of the stopped-flow apparatus is 1 ms. The applied flow rate was 12 mL/sec and 40 μL shot volumes were mixed at 1:1 ratio. 1–4 μ*M* enzymes in 20 m*M* CABS (Sigma-Aldrich, St. Louis, MO), 10 m*M* $CaCl_2$ pH 11.0 were mixed with 100 m*M* Tricine, 10 m*M* $CaCl_2$ pH 8.0 and the fluorescence emission intensity increase was monitored. The rate of the conformational change was measured with this setup in the 5–38°C temperature range in 3°C increments. The pHs of the buffers were adjusted at room temperature to different pH values to give the final value pH 8.0 ± 0.1 pH (and pH 11.0 ± 0.1) at the different experimental temperatures.

Temperature-jump/stopped-flow experiments

Measurements were carried out on a temperature-jump/stopped-flow instrument developed in our laboratory.[21] The enzyme was kept at 20°C until mixing with the pH 8.0 buffer, which flows through a heated loop. The temperature of the cuvette is also controlled by another heating element (Supertech, Pécs, Hungary) to ensure that the temperature of the mixture and the reaction chamber is equal. Twenty microliter enzyme in 20 m*M* CABS, 10 m*M* $CaCl_2$ pH 11.0 was mixed with 100 μL 100 m*M* Tricine, 10 m*M* $CaCl_2$ pH 8.0 and the fluorescent emission change was detected. The pHs of the buffers were adjusted at room temperature to yield the final value at the different experimental temperatures as described above. The 1:5 mixing ratio enables a greater temperature-jump and at the same time allows keeping the enzyme at non-denaturing temperatures until the reaction. Throughout the applied temperature range both the loop and the cuvette were overheated compared with the theoretical formula $(1 \times 20°C + 5 \times T_{loop})/6 = T_{cuvette}$ to compensate for the heat-loss of the system. Temperature calibration of the setup was performed by measuring the fluorescence intensity of NATA (Sigma-Aldrich, St. Louis, MO) at different temperatures generated with the temperature-jump/stopped-flow method[21] taking advantage of the temperature dependence of fluorescence.[24] Briefly, NATA was loaded into the cold syringe and rapidly mixed with hot buffer pushed through the heating loop inserted between the other syringe and the mixing chamber. Change in fluorescence intensity of NATA in the cuvette indicated that the temperature of the reaction mixture and the cuvette were not identical right after mixing and temperature reequilibration occurred in the cuvette. Fluorescence intensity decrease indicates that the reaction mixture was colder than the cuvette and the solution warmed up in the cuvette and *vice versa*. Temperature of the heating loop and the cuvette was adjusted so that the fluorescence intensity of NATA did not change after mixing which indicates that the temperature of the mixture was equal to the temperature of the cuvette.

Determination of dependence of the rate constants on the relative external viscosity

Stopped-flow measurements were carried out at 20.0°C using buffers 10 m*M* CABS, 5 m*M* $CaCl_2$, pH 11.0 and

50 m*M* Tricine, 5 m*M* $CaCl_2$, pH 8.0 supplemented with viscogen to yield different relative viscosities. Maltose (Sigma-Aldrich, St. Louis, MO) was applied as a viscogen in the concentration range of 0–1.46 *M* resulting in relative viscosities of 1–8.18.[25] Maltose increases the relative viscosity to the greatest extent while reducing the dielectric constant of the solvent the least as compared with other frequently used viscogens, eg fructose[26] and ethylene glycol.[25] The concentration of the buffers was reduced compared with the other measurements as ionic strength influences the viscosity. Other experimental settings were the same as described in the *Stopped-Flow Measurements section*.

Kinetic and Thermodynamic Analysis

5–8 recorded transient traces were averaged and analyzed by fitting to single or double exponential functions using the KinTek software (KinTek, Austin, TX) and OriginLab v7.5 (OriginLab, Northampton, MA). Thermodynamic profiles were analyzed by fitting exponential functions following $y = a\exp(b/x)$ to the plots of the observed rate constants (k) versus temperature (T). The parameters of the fitted function can be directly corresponded to the parameters of the Arrhenius equation without linearization ($y = k$, $a = A$, $b = -E_a/R$, $x = T$).

Temperature dependence of a reaction rate constant is described by the Arrhenius equation[27]:

$$k = A\exp(-E_a/RT) \tag{1}$$

where k is the rate constant, A is the preexponential term, E_a stands for the activation energy of the process, R is the gas constant and T is the absolute temperature. Kramers' theory is a conventional theoretical approach to describe the effect of friction on the rate constants of unimolecular reactions in the condensed phase.[28] In this model the chemical reaction is modeled by a particle with a diffusive one-dimensional motion from a potential well over a barrier. On the basis of Kramers' rate theory, the preexponential term of the Arrhenius equation contains a friction parameter, which is determined dominantly by viscosity and the rate constant is inversely proportional to this friction.

Ansari et al.[22] modified this approach for proteins by separating the friction into two sources of friction because only a part of the protein interacts with the solvent molecules. One of these terms is the friction of the solvent (external friction) restraining the motion of the atoms on the surface of the protein and the other term is the internal friction of the protein hindering the motion of the protein atoms relative to each other. The following equation was stated to describe this model:

$$k = \frac{C}{\sigma + \eta}\exp(-E_a/RT) \tag{2}$$

where η is the external (solvent) viscosity and σ is a parameter with units of viscosity that determines the internal friction of the protein, henceforth referred to as internal viscosity. C includes the viscosity independent parameters. The solvent friction, according to Stokes' law, is proportional to the solvent viscosity. On the basis of this analogy, the internal molecular friction can also be referred to as the internal viscosity of the protein, and this viscosity-like parameter has units of viscosity. Still, this is not to be considered as a general parameter of the protein, but it is coupled to a specific conformational transition in the molecule.

Assuming that the activation energy does not depend on the viscosity at constant temperature, modification of Eq. (2) results in:

$$k = \frac{C'}{\sigma + \eta} \tag{3}$$

where C′ includes $C\exp(-E_a/RT)$. The linearized form of Eq. (3) will then be the following:

$$\frac{1}{k} = \frac{\eta}{C'} + \frac{\sigma}{C'} \tag{4}$$

As a consequence, plotting $1/k$ against the external viscosity gives a linear function, and internal viscosity of the protein can be deduced from its intercept multiplied by the reciprocal of the slope. In other words, at constant temperature [Eq. (4)], the internal viscosity can be calculated by the extrapolation of the rate constant to zero external viscosity ($\eta = 0$ cP):

$$\sigma = \frac{C'}{k} - \eta \tag{5}$$

Thus by measuring the rate of the conformational change as a function of the relative viscosity of the reaction buffer, the internal viscosity of a protein can be determined.

RESULTS

Enzymatic Activity of Human Trypsin 4 and Its Mutants at Position 193

The experiments described here utilize human trypsin 4 and its variants in which arginine 193 was substituted with a glycine, alanine, phenylalanine or a tyrosine residue. To test whether the enzymatic activity of these variants is affected by the mutations, their catalytic activity of amide bond hydrolysis was measured on Z-Gly-Pro-Arg-pNA substrate. The determined values for the Michaelis-Menten parameters are summarized in Table I. Our data show that the mutations caused only slight changes in the k_{cat} and K_m values. The greatest change in the K_m is within 50% and for the k_{cat} value it does not exceed 30%. The k_{cat} value increases upon replacement of the glycine with a more bulky residue, and the degree of this increase correlates with the size of the sidechain. The same observation holds also for the K_m value. The greatest change in the k_{cat}/K_m value upon these amino acid substitutions is 30%, thus these site 193 variants can all be considered as active enzymes. These results

TABLE I. Hydrolysis of Z-Gly-Pro-Arg-pNA Amide Substrate by Wild-Type Human Trypsin 4 and its Mutants at Position 193

	k_{cat} (s^{-1})	K_m (μM)	k_{cat}/K_m (s^{-1} μM^{-1})
R193G	110 ± 10	13.5 ± 2.5	8.17 ± 1.68
R193A	124 ± 4	19.8 ± 3.2	6.23 ± 1.02
WT	158 ± 8	25.2 ± 0.6	6.27 ± 0.36
R193F	162 ± 5	27.4 ± 6.7	5.90 ± 1.45
R193Y	133 ± 6	21.3 ± 6.1	6.21 ± 1.80

Assays were performed in 50 m*M* Tricine, 10 m*M* $CaCl_2$ pH 8.0 at 20.0°C as described under Materials and Methods. The values of the Michaelis–Menten parameters represent the mean ± SEM of three measurements. Errors of k_{cat}/K_ms were calculated taking the propagation of error into account.

indicate that both substrate binding and catalysis of hydrolysis of Z-Gly-Pro-Arg-pNA are only moderately affected by these mutations.

Kinetic and Thermodynamic Analysis of the Conformational Change During pH-Jump Activation

The rate of the conformational rearrangement in the course of activation was measured by monitoring the intrinsic fluorescent intensity change of the proteins in pH-jump stopped-flow experiments. In these experiments one of the syringes of the stopped-flow contained the enzyme in a buffer with a relatively low buffer capacity at pH 11 and the other syringe contained a buffer with high buffer capacity at pH 8.0. The pH of the solution after mixing was 8.0 ± 0.1. This pH-jump initiated the structural rearrangement reaction which was monitored by the tryptophan fluorescence change. Our data show that the rates of the conformational change are affected by the mutations at position 193. The rate constants at 20.0°C for the site 193 variants are as follows: $k_{R193G} = 1.66\ s^{-1}$, $k_{R193A} = 0.20\ s^{-1}$, $k_{WT} = 0.077\ s^{-1}$, $k_{R193Y} = 0.13\ s^{-1}$, $k_{R193F} = 0.090\ s^{-1}$. We note that burst phases were detected for wild type human trypsin 4, the R193Y, and the R193F mutants with amplitudes between 11–16% of the total fluorescence change and rate constants 7–17 times larger than that of the analyzed dominant phases.

Furthermore, to investigate the thermodynamics of the conformational change during activation, temperature dependence of the rate constants was measured. Thermodynamic parameters for the conformational change were derived from the non-linearized Arrhenius plots (k plotted against T) and are summarized in Table II. The Arrhenius plots (ln k plotted against $1/T$) were linear in the temperature range of 5–45°C (Fig. 2). Eyring plots were also fitted to the data, in which the preexponential factor is temperature dependent and the statistical significance (χ^2) of the fitting did not change significantly. In addition, no significant differences were found in the reliability of fitting when the Kramers' equation corrected with the temperature dependence of the viscosity of water was fitted to the data. Our most important finding is that the Arrhenius plots are parallel for the site 193 variants of human trypsin 4. It indicates that the activation energy (E_a) of the conformational transition is not affected by the amino acid substitutions. Thus exponents "*b*" of the fitted exponential functions (slope of the linearized Arrhenius plots) are practically the same (Fig. 2, Table II). The largest difference in the activation energies was found between wild type and the R193F mutant human trypsin 4 amounting to 4%. The activation energies of the rest of the mutants differed only by 0.8%–2%. In contrast, the intercepts of the linearized Arrhenius plots for these enzyme variants differ significantly, suggesting that these mutations selectively alter the preexponential term of the Arrhenius equation. The greatest difference in the preexponential terms is 26-fold found for the R193G and R193F mutants (Table II).

By developing a novel temperature-jump/stopped-flow setup, we were able to extend the Arrhenius plots up to 60°C. Deviations from the linear function could be observed above 45°C which indicate another reaction step. It has to be noted, however, that denaturation happens on the ten sec time scale at 45–60°C, which could be detected by the decline of the fluorescence intensity while the activation process is more than an order of magnitude faster at these temperatures.

To investigate the effects of these mutations on the preexponential term in more detail, we also performed experiments in which the relative viscosity of the buffers was varied. The question was if the rate constant of a conformational change decreases as the solvent viscosity is increased as predicted by the Kramers' theory. To answer this question pH-jump stopped-flow measurements were carried out on the wild type enzyme and its R193G and R193A mutants in buffers of different relative viscosity from 1 to 8.18 at 20°C. The increased solvent viscosity caused dramatic effect on the rate constants of the pH-jump induced conformational change of the examined mutants (Fig. 3): at relative external viscosity of 2 the rate constants decreased by 45% for the R193G variant, by 36% for the R193A mutant and by 27% for the wild type enzyme. We found hyperbolic relations between the observed rate constants and the external viscosity for the studied mutants which confirm the validity of Kramers' theory applied to this conformational change between two structurally definite conformers. Since the fluorescence change accompanying the conformational transition was relatively slow in the case of wild type enzyme and at high maltose concentrations a slow signal decrease masked the increasing signal, the highest applied relative external viscosity was 2.2 in case of this enzyme. Reciprocal values of the rate constants were plotted against the relative external solvent viscosity and linear functions were fitted to the data (Fig. 4). The parameters of the fitted linear functions and internal viscosities, calculated according to Eq. (5), are presented in Table III. Our data show that the relative internal viscosity of the R193A mutant is 3-fold greater compared with the R193G mutant, the relative internal viscosity of the arginine possessing counterpart is 6-fold greater relative to the glycine mutant and is 2-fold greater than

TABLE II. Thermodynamic Parameters Derived From the Nonlinearized Arrhenius Plots of Wild-Type Human Trypsin 4 and its Mutants at Position 193

	R193G	R193A	WT	R193F	R193Y
b^*	$-(10.4 \pm 0.4) \times 10^3$	$-(10.7 \pm 0.2) \times 10^3$	$-(10.8 \pm 0.3) \times 10^3$	$-(10.3 \pm 0.2) \times 10^3$	$-(10.5 \pm 0.3) \times 10^3$
E_a (kJ mol^{-1})	86.5 ± 3.4	88.7 ± 1.6	89.5 ± 2.4	85.7 ± 1.9	87.2 ± 2.7
$a^* = A$	3.95×10^{15}	1.12×10^{15}	6.50×10^{14}	1.49×10^{14}	4.40×10^{14}

The rate of the conformational change during pH-jump activation was measured in a wide temperature range with a stopped-flow apparatus monitoring the intrinsic fluorescent emission change of the proteins. Experimental conditions were as described under Materials and Methods. Rate constants were plotted against temperature, and the exponential function following $*y = a \exp(b/x)$ was fitted to the data. Thermodynamic parameters were derived from the parameters "a" and "b" of the fitted functions as described under Materials and Methods. Values represent the mean and ± SEM of the parameters for the fitted exponential functions.

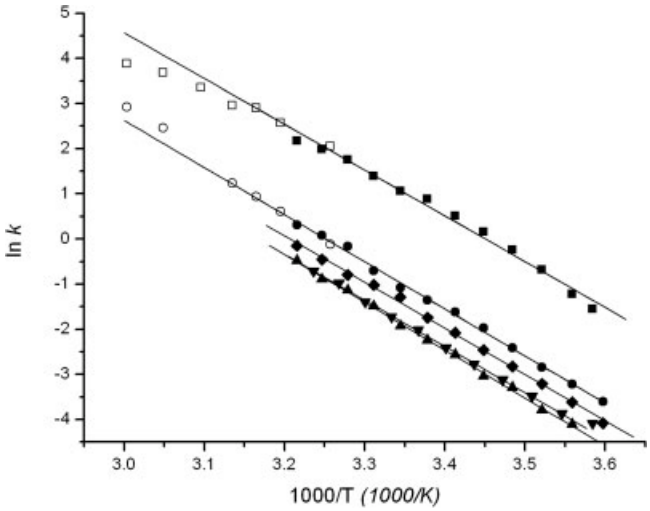

Fig. 2. Arrhenius plots (ln k plotted against 1/T) for the rate constants of the conformational change during activation for wild type human trypsin 4 (▲) and its site 193 variants R193G (■ and □), R193A (● and (○), R193F (▼) and R193Y (♦). The conformational change was triggered by a pH-jump and its rate constant was measured using a stopped-flow and a temperature-jump/stopped-flow apparatus monitoring the fluorescent emission change. The rate of the conformational change was measured with a conventional setup in the 5–38°C temperature range in 3°C increments (closed marks). In the 34–60°C temperature range a novel temperature-jump/stopped-flow equipment developed in our laboratory was applied to extend the Arrhenius plots of R193G and R193A variants (open marks). Experimental conditions were as described in *Materials and Methods*. Thermodynamic parameters were determined from the parameters of the fitted exponential functions following y = a exp (b/x) as described under *Materials and Methods*.

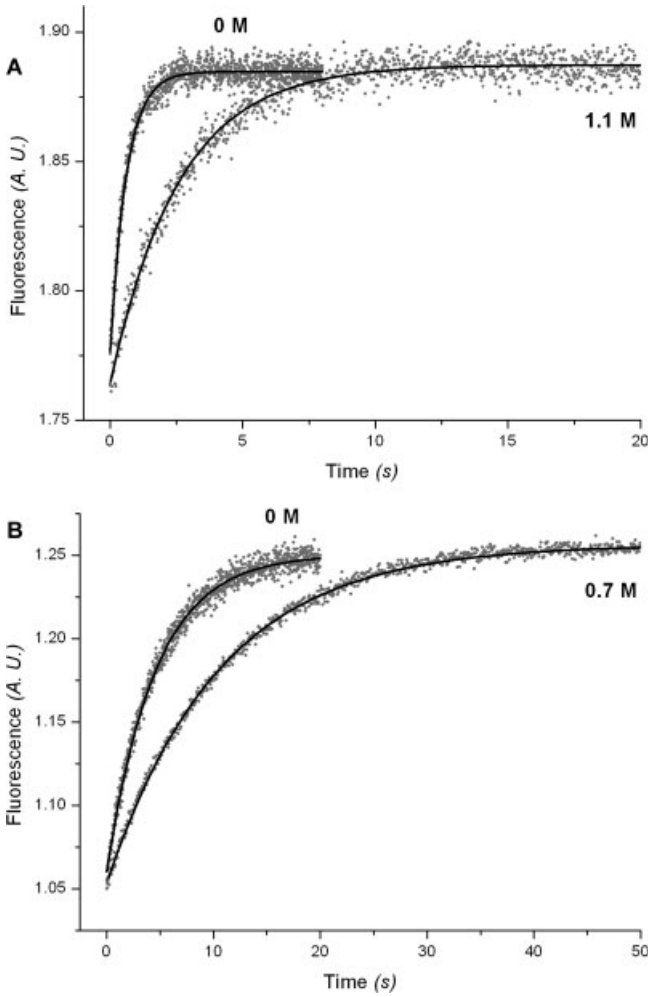

Fig. 3. Stopped-flow records on exposing human trypsin 4 R193G (**A**) and R193A mutant (**B**) to a pH-jump from pH 11.0 to pH 8.0 in buffers of different relative viscosity. Both buffers were supplemented with a given concentration of maltose to yield different relative external viscosities. Experimental conditions are described in *Materials and Methods*. The fluorescent emission change was monitored, and single exponentials were fit to the recorded traces. The rate constant of the conformational transition decreased as the solvent viscosity was increased by the viscogen. The observed rate constants for the presented traces are the following: $k_{R193G\ rel\ visc=1} = 1.65\ s^{-1}$, $k_{R193G\ rel\ visc=4.4} = 0.39\ s^{-1}$, $k_{R193A\ rel\ visc=1} = 0.22\ s^{-1}$, and $k_{R193A\ rel\ visc=2.2} = 0.095\ s^{-1}$.

that of the alanine mutant ($\sigma_{R193G} = 0.27$, $\sigma_{R193A} = 0.81$, $\sigma_{WT} = 1.67$). These data clearly suggest that a bulkier amino acid at the hinge region locally increases the internal molecular viscosity in the protein resulting in an increase of the steric hindrance for a specific conformational change.

DISCUSSION

The major goal of our work was to determine if the rate and thermodynamics of the conformational change during pH-jump induced activation of trypsin is affected by the character of the residue at one of the hinge positions. We therefore investigated the temperature and viscosity dependence of the conformational change during activation in human trypsin 4 and its R193G/A/F/Y mutants in pH-jump stopped-flow experiments. These amino acids at position 193 allowed different degree of

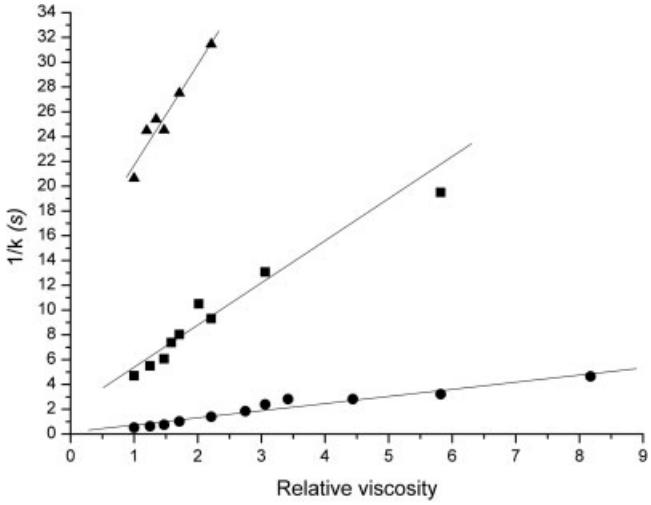

Fig. 4. Dependence of the rate constants of the conformational change during activation on the external viscosity for the wild type human trypsin 4 (▲) and its R193A (■) and R193G (●) mutants. Stopped-flow measurements were carried out at 20.0 °C using buffers supplemented with 0–1.46*M* maltose as viscogen to yield different relative viscosities from 1 to 8.18 as described in "Materials and methods". The rate constants presented are the averages of three independent data sets each originating from 8–12 recorded transients for each mutant. 1/k was plotted against the relative external viscosity and linear functions were fitted to the measured data. Relative internal viscosities were calculated from the intercept and slope of the linear fits according to Eq. (4).

TABLE III. Relative Internal Viscosity of Wild Type Human Trypsin 4 and its R193G and R193A Mutant Derived From the Viscosity Dependence of the Reaction Rate of the Conformational Change During Activation

	R193G	R193A	WT
Slope	0.575 ± 0.05	3.07 ± 0.25	8.13 ± 1.09
Intercept	0.156 ± 0.187	2.48 ± 0.67	13.56 ± 1.67
Relative internal viscosity	0.27	0.81	1.67

Rates of the conformational change during activation were measured in pH-jump stopped flow experiments applying buffers of different viscosity from 1 to 8.18. Experimental conditions were as described under Materials and Methods. 1/ks were plotted against the relative external viscosity and linear functions were fitted to the data. The internal viscosity of the proteins was calculated according to Eq. 4. Values for the intercepts and slopes represent the mean and standard deviation of the fitted linear functions. The viscosity dependence of the reaction rate constants were measured at 20.0°C. As the viscosity of water is 1 cP at 20.0°C, the value of the calculated internal viscosity in cP is the same as the relative value.

freedom for the hinge around which the conformational rearrangement occurs.

Human trypsin 4 possesses 5 tryptophan residues: Trp221 is part of segment 216–223, while Trp141 and Trp215 are located in the close vicinity of peptide segments 142–152 and 216–223 that are involved in the conformational transition of activation. These native tryptophans are appropriate probes to monitor the structural rearrangement induced by the pH-jump activation, as their fluorescence intensity increases significantly during this process. The tryptophan-based detection method has several advances compared with ligand-binding assays (e.g. proflavine binding): this reaction follows first order kinetics, intrinsic fluorescence detection gives a direct read-out, and it even has greater sensitivity thus requiring less protein.

Trypsin undergoes a reversible conformational change during pH-jump from an inactive zymogen-like structure at pH 11.0 to the active conformation at pH 8.0. Therefore, the observed rate constant measured by monitoring the intrinsic fluorescence change of the protein is the sum of the forward and reverse rate constant for the reaction. The equilibria at pH 8.0 is highly shifted towards the forward direction as it was shown for rat trypsin,[29] thus the contribution of the reverse rate constant to the observed rate constant is negligible. As a consequence, the transition is practically irreversible, and the observed rate constant can be considered as the forward rate constant for the process.

Activation domain peptides are bordered by glycine residues (Gly19, Gly142, Gly184, Gly193 and Gly216) which act as hinges in the process of activation indicated by the large Φ and/or Ψ dihedral angle transitions that occur at these positions.[12] The values for the peptide backbone dihedral angles at Gly193 are $\Phi = -148.7^\circ$ and $\Psi = 18.1^\circ$ in bovine trypsinogen (PDB ID: 1tgb), while in bovine trypsin (PDB ID: 2 ptn) these values change to $\Phi = 105.4^\circ$ and $\Psi = -19.1^\circ$. The atomic structure of human trypsin 4 complexed with benzamidine has been resolved and it was shown that in spite of the G193R mutation, the overall fold of the molecule is highly similar to that of human trypsin 1 having a glycine at this position.[20] The effect of the G193A mutation was studied in thrombin, and based on the atomic structure of this mutant neither did this mutation cause structural perturbation in the overall conformation of the peptide backbone, only slight changes were detected at the site of mutation.[30] Similarly, in computer modeling studies of G193E (G555E) mutant FactorXI no significant conformational changes were found in the peptide backbone.[31] These data suggest that substitution of glycine193 with an amino acid having a bulkier side chain does not perturb significantly the overall fold of the molecule. Although there is only a slight structural change in the peptide backbone conformation, we supposed that some other dynamics-related physical parameter to be characterized might affect the rate of conformational change during activation in trypsin site 193 variants.

In the presented study we mutated R193 of human trypsin 4 to glycine, alanine, phenylalanine and tyrosine. These mutations did not cause large perturbation in the steady state enzyme kinetic values on Z-Gly-Pro-Arg-pNA substrate (Table I). Besides from being one of the hinge residues during the activation, residue 193 has an important role in substrate binding and enzyme catalysis. The amido group of residue at position 193 is part of the oxyanion hole which stabilizes the developing tetrahedral intermediates during catalysis,[32,33] thus the sub-

stitution of Gly193 slightly influences the k_{cat} value. These results suggest that the substrate binding pocket and the geometry of the oxyanion hole are not perturbed significantly by these mutations. Our results are confirmed by previous studies showing that the Gly193Arg point mutation only slightly changes the steady-state activity of the enzyme on small synthetic substrates.[16,19]

The rate of the conformational transition during pH-jump induced activation of wild type and R193G/A/F/Y mutant human trypsin 4 was measured by monitoring the intrinsic fluorescent intensity change of the proteins in stopped-flow experiments. The rates of the conformational change are influenced by the mutations at position 193, and the values correlate with the size of the side-chain. The temperature dependences of the rate of pH induced activation were also determined. Strikingly, we found that the Arrhenius plots of the reactions were parallel for all of the mutants. This phenomenon was investigated in a wide temperature range (between 5°C and 60°C) applying a new stopped-flow equipment called temperature-jump/stopped-flow developed in our lab.[21] The wide temperature range allowed us to improve the reliability that the Arrhenius plots are parallels. These results suggest that activation energies are identical and the thermodynamic parameters for these trypsin mutants differ only in the preexponential term. Further important observation is that the larger the size of the substituted amino acid side chains at position 193 the smaller the value of the preexponential term. This aspect of the results indicates that restricting the conformational freedom of the hinge affects the preexponential term and not the activation energy.

Eyring–Polányi transition state theory is a general model and it is adequate only for the description of temperature dependence of reactions in the gas phase. Biomolecular reactions take place in the condensed phase and have complex multidimensional potential energy surfaces,[34] therefore it is required to introduce a transmission coefficient to the preexponential term of the generalized transition state theory (reviewed by Garcia-Viloca et al.[35]). Kramers' theory is an appropriate and relatively simple approach for the description of reactions of complex molecules in the condensed phase.[36] As stated in the work of Frauenfelder and coworkers, if the reaction rate depends strongly on solvent viscosity, data can be assessed using Kramers' theory. In the work of Beece et al. the ligand binding of protoheme and myoglobin was studied in solvents in which the viscosity was varied over a wide range postulating that the solvent affects the protein reaction predominantly through solvent viscosity.[37] This experimental approach is in agreement with the idea that barriers governing the transition between two states in a protein have dynamic origins. The transition state theory is valid only in a limited region of solvent viscosity, below 1 mP, thus the application of this theory to reactions even in aqueous solutions is uncertain, and rather Kramers' theory is appropriate. The phenomenon described in our paper, that the rate constant of a reaction is inversely proportional to the solvent viscosity is consistent with Kramers' theory.

To analyze the effect of the preexponential term on the rate of the structural rearrangement in detail, we examined whether the rate of the conformational transition is affected by the viscosity of the solvent. Kramers' equation predicts a hyperbolic dependence of the rate constants on solvent viscosity [Eq. (4)]. We measured the rate of the conformational change in buffers of different relative viscosity using maltose as a viscogen. Our data clearly show that the rate constant depends on the viscosity of the solvent (Fig. 3), even at relatively low viscogen concentrations where the perturbation of protein stability and charged-charged interactions by the slightly decreased dielectric constant of the solvent were insignificant. There are several other reports on the viscosity dependence of the rate of diverse protein reactions showing that the rate decrease upon addition of small molecular weight viscous cosolvents (eg glycerol, ethylene glycol, sucrose) is due to the increased solvent viscosity and not the result of either a change in the dielectric constant or ionic strength of the reaction buffer, the alteration of osmotic pressure, a change in the hydration of charged groups or chemical-potential change arising from the solvent-cosolvent interaction,[37–39] especially at low concentrations of viscogen as we applied. Furthermore, we found that the relation is hyperbolic, thus 1/k plotted against the relative external viscosity yields a linear function (Fig. 4) which strongly indicates that Kramers' theory is an appropriate framework for the description of rates of enzyme conformational transitions under native conditions.

On the basis of the work of Ansari et al. [Eq. (2)],[22] the internal viscosity of a protein can be calculated by determining the dependence of the rate constant on the external viscosity and extrapolating to zero external viscosity [Eq. (5)]. We determined the viscosity dependence of the rate constant using the wild type enzyme and its R193G and R193A mutant and linear functions were fitted to the plot of 1/k versus relative external viscosity. We found that both the slope and intercept of these linear functions are different in these mutants (Fig. 4). The calculated internal viscosity of the alanine mutant is increased threefold as compared with the glycine mutant, and this parameter of the wild type enzyme is increased twofold relative to the alanine mutant and 6-fold compared with the glycine possessing counterpart (Table III). We conclude that the bulkier sidechain of alanine allows less conformational freedom for the peptide backbone in the conformational transition as compared with glycine which can be revealed as an increase in a viscosity-like parameter defined as internal viscosity.

It is also interesting, that this viscosity-like parameter is around the viscosity of water at 20.0°C which indicates relatively low restriction by the hinge region. Ansari et al. determined the value of σ to be 4.1 cP in myoglobin related to the conformational change after ligand dissociation.[22] This parameter is larger than what we found in trypsin during its conformational change of

activation. The relatively ordered water molecules in the heme pocket of myoglobin may play an important role in the studied reaction which may increase the value of internal viscosity. Nevertheless, it has to be emphasized that internal viscosity is not a general parameter of the protein but it is associated with a specific conformational rearrangement.

In summary, our results illustrate that a specific conformational rearrangement of an enzyme is a Kramers' type reaction under native conditions. Furthermore, our data show that internal viscosity can be modified specifically by mutations, in this way modulating the mobility of the hinge around which the structural change occurs.

ACKNOWLEDGMENT

We are grateful for the excellent technical assistance of Vilmosné Énekes.

REFERENCES

1. Birktoft JJ, Kraut J, Freer ST. A detailed structural comparison between the charge relay system in chymotrypsinogen and in α-chymotrypsin. Biochemistry 1976;15:4481–4485.
2. Kossiakoff AA, Chambers JL, Kay LM, Stroud RM. Structure of bovine trypsinogen at 1.9 Å resolution. Biochemistry 1977;16: 654–664.
3. Huber RBW. Structural basis of the activation and action of trypsin. Acc Chem Res 1978;11:114–122.
4. Guex N, Peitsch MC. SWISS-MODEL and the Swiss-PdbViewer: an environment for comparative protein modeling. Electrophoresis 1997;18:2714–2723.
5. Fehlhammer H, Bode W, Huber R. Crystal structure of bovine trypsinogen at 1.8 Å resolution. II. Crystallographic refinement, refined crystal structure and comparison with bovine trypsin. J Mol Biol 1977;111:415–438.
6. Bode W, Schwager P, Huber R. The transition of bovine trypsinogen to a trypsin-like state upon strong ligand binding. The refined crystal structures of the bovine trypsinogen-pancreatic trypsin inhibitor complex and of its ternary complex with Ile-Val at 1.9 Å resolution. J Mol Biol 1978;118:99–112.
7. Fersht AR, Renard M. pH dependence of chymotrypsin catalysis. Appendix: substrate binding to dimeric α-chymotrypsin studied by X-ray diffraction and the equilibrium method. Biochemistry 1974;13:1416–1426.
8. Stoesz JD, Lumry RW. Refolding transition of α-chymotrypsin: pH and salt dependence. Biochemistry 1978;17:3693–3699.
9. Heremans L, Heremans K. Raman spectroscopic study of the changes in secondary structure of chymotrypsin: effect of pH and pressure on the salt bridge. Biochim Biophys Acta 1989;999: 192–197.
10. Verheyden G, Mátrai J, Volckaert G, Engelborghs Y. A fluorescence stopped-flow kinetic study of the conformational activation of α-chymotrypsin and several mutants. Protein Sci 2004;13: 2533–2540.
11. Fersht AR, Requena Y. Equilibrium and rate constants for the interconversion of two conformations of α-chymotrypsin. The existence of a catalytically inactive conformation at neutral pH. J Mol Biol 1971;60:279–290.
12. Brünger AT, Huber R, Karplus M. Trypsinogen-trypsin transition: a molecular dynamics study of induced conformational change in the activation domain. Biochemistry 1987;26:5153–5162.
13. Wroblowski B, Diaz JF, Schlitter J, Engelborghs Y. Modelling pathways of α-chymotrypsin activation and deactivation. Protein Eng 1997;10:1163–1174.
14. Mátrai J, Verheyden G, Kruger P, Engelborghs Y. Simulation of the activation of α-chymotrypsin: analysis of the pathway and role of the propeptide. Protein Sci 2004;13:3139–3150.
15. Szilágyi L, Kénesi E, Katona G, Kaslik G, Juhász G, Gráf L. Comparative *in vitro* studies on native and recombinant human cationic trypsins. Cathepsin B is a possible pathological activator of trypsinogen in pancreatitis. J Biol Chem 2001;276:24574–24580.
16. Szmola R, Kukor Z, Sahin-Tóth M. Human mesotrypsin is a unique digestive protease specialized for the degradation of trypsin inhibitors. J Biol Chem 2003;278:48580–48589.
17. Sahin-Tóth M. Human mesotrypsin defies natural trypsin inhibitors: from passive resistance to active destruction. Protein Pept Lett 2005;12:457–464.
18. Tóth J, Gombos L, Simon Z, Medveczky P, Szilágyi L, Gráf L, Málnási-Csizmadia A. Thermodynamic analysis reveals structural rearrangement during the acylation step in human trypsin 4 on 4-methylumbelliferyl 4-guanidinobenzoate substrate analogue. J Biol Chem 2006;281:12596–12602.
19. Medveczky P, Tóth J, Gráf L, Szilágyi L. The effect of Arg193 on the enzymatic properties of human brain trypsin. In: Abbasi A,Ali SA, editors. Protein structure-function relationship. Karachi, Pakistan: BCC&T Press; 2003. pp 41–53.
20. Katona G, Berglund GI, Hajdu J, Gráf L, Szilágyi L. Crystal structure reveals basis for the inhibitor resistance of human brain trypsin. J Mol Biol 2002;315:1209–1218.
21. Kintses B, Simon Z, Gyimesi M, Tóth J, Jelinek B, Niedetzky Cs, Kovács M, Málnási-Csizmadia A. Enzyme kinetics above denaturation temperature: a temperature-jump/stopped-flow apparatus. Biophys J 2006;91:4605–4610.
22. Ansari A, Jones CM, Henry ER, Hofrichter J, Eaton WA. The role of solvent viscosity in the dynamics of protein conformational changes. Science 1992;256:1796–1798.
23. Jameson GW, Roberts DV, Adams RW, Kyle WS, Elmore DT. Determination of the operational molarity of solutions of bovine α-chymotrypsin, trypsin, thrombin and factor Xa by spectrofluorimetric titration. Biochem J 1973;131:107–117.
24. Lakowicz JR. Principles of fluorescence spectroscopy, 2nd ed. New York, USA: Kluwer; 1999.
25. Weast RC, editor. CRC handbook of chemistry and physics, 69th ed. Boca Raton, Florida: CRC; 1988.D-236 p.
26. Fuchs K, Kaatze U. Dielectric spectra of mono- and disaccharide aqueous solutions. J Chem Phys 2002;116:7137–7144.
27. Arrhenius S. Über die Reaktionsgeschwindigkeit bei der Inversion von Rohzucker durch Säuren. Z Phys Chem 1889;4:226–248.
28. Kramers HA. Brownian motion in a field of force and the diffusion model of chemical reactions. Physica 1940;7:284–304.
29. Hedström L, Lin TY, Fast W. Hydrophobic interactions control zymogen activation in the trypsin family of serine proteases. Biochemistry 1996;35:4515–4523.
30. Bobofchak KM, Pineda AO, Mathews FS, Di Cera E. Energetic and structural consequences of perturbing Gly-193 in the oxyanion hole of serine proteases. J Biol Chem 2005;280:25644–25650.
31. Zivelin A, Ogawa T, Bulvik S, Landau M, Toomey JR, Lane J, Seligsohn U, Gailani D. Severe factor XI deficiency caused by a Gly555 to Glu mutation (factor XI-Glu555): a cross-reactive material positive variant defective in factor IX activation. J Thromb Haemost 2004;2:1782–1789.
32. Henderson R. Structure of crystalline α-chymotrypsin. IV. The structure of indoleacryloyl-α-chyotrypsin and its relevance to the hydrolytic mechanism of the enzyme J Mol Biol 1970;54:341–354.
33. Robertus JD, Kraut J, Alden RA, Birktoft JJ. Subtilisin: a stereochemical mechanism involving transition-state stabilization. Biochemistry 1972;11:4293–4303.
34. Frauenfelder H, Sligar SG, Wolynes PG The energy landscapes and motions of proteins. Science 1991;254:1598–1603.
35. Garcia-Viloca M, Gao J, Karplus M, Truhlar DG. How enzymes work: analysis by modern rate theory and computer simulations. Science 2004;303:186–195.
36. Frauenfelder H, Wolynes PG. Rate theories and puzzles of hemeprotein kinetics. Science 1985;229:337–345.
37. Beece D, Eisenstein L, Frauenfelder H, Good D, Marden MC, Reinisch L, Reynolds AH, Sorensen LB, Yue KT. Solvent viscosity and protein dynamics. Biochemistry 1980;19:5147–5157.
38. Schlarb-Ridley BG, Mi H, Teale WD, Meyer VS, Howe CJ, Bendall DS. Implications of the effects of viscosity, macromolecular crowding, and temperature for the transient interaction between cytochrome f and plastocyanin from the cyanobacterium *Phormidium laminosum.*. Biochemistry 2005;44:6232–6238.
39. Almagor A, Yedgar S, Gavish B. Viscous cosolvent effect on the ultrasonic absorption of bovine serum albumin. Biophys J 1992;61:480–486.